Journal of Sound and Vibration 399 (2017) 244–256

Contents lists available at ScienceDirect

Journal of Sound and Vibration

journal homepage: www.elsevier.com/locate/jsvi

Limits on the power available to harvest from broadband random excitation

D.H. Hawes *, R.S. Langley

Cambridge University Engineering Department, Trumpington Street, Cambridge CB2 1PZ, UK

ARTICLE INFO

Article history:
Received 13 October 2016
Received in revised form
23 February 2017
Accepted 27 March 2017
Handling Editor: MP Cartmell
Available online 7 April 2017

Keywords:
Energy harvesting
Piezoelectric
Electromagnetic
White noise

ABSTRACT

With the large diversity in energy harvesters aiming to extract maximum power from broadband excitations, it is important to know what the maximum power achievable is. This paper derives new upper bounds on the available power for a harvester with general nonlinear stiffness coupled to a nonlinear electrical circuit. White noise base excitations are known to input power proportional to the total oscillating mass of the system and the magnitude of the spectral density of the noise regardless of the details of the oscillating system. This power is split between undesirable mechanical damping and useful electrical dissipation with the form of the stiffness profile and device parameters determining the relative proportions in each dissipation mechanism. An upper bound on electrical power is sought and, provided certain conditions are met, shown to be a simple function of relatively few system parameters and, importantly, independent of the stiffness profile or electrical nonlinearity.

The benefits of knowing the upper limits on power are threefold: to guide optimal harvester design, to assess how close to optimal current devices are and to provide a preliminary estimation of the harvester mass necessary in a given operating environment for a given power requirement.

1. Introduction

As technology develops, the power consumption of electronic devices is decreasing rapidly. Consequently, there is substantial interest in harvesting energy from ambient sources, such as vibration, in order to power small-scale wireless devices where battery replacement or wiring is impractical or unnecessary. The vibrations of an engineering application can be used to excite an electromechanical oscillator that converts the kinetic energy into electrical energy. A number of energy conversion techniques and system designs have been investigated and are comprehensively reviewed in [1–4].

The ability of an energy harvester to extract the maximum power from a given excitation will strongly depend on the characteristics of the excitation. A large proportion of applications will be dominated by harmonic vibrations at one or more fixed or time-varying frequencies and substantial research has been undertaken to develop optimal energy harvesters under these conditions [3,5–7]. However, many applications will vibrate randomly with a broad frequency range often modelled as white [8–19] or other [11,12,20–27] noise.

It is critical in energy harvesting to investigate what the maximum power available from a given excitation is and what type of system can achieve it. For a general force input, an analysis of input energy subtracted by power dissipated under

* Corresponding author.
E-mail address: dhh29@cam.ac.uk (D.H. Hawes).

http://dx.doi.org/10.1016/j.jsv.2017.03.036
0022-460X/

various constraints can be made to devise a strategy for maximum power transfer [28–30]. This is effective for deterministic or relatively consistent vibrations, but less capable of handling random excitation. Additionally, unphysical or difficult to realise responses are often found to provide the optimal velocity profile although [30,31] suggest a type of system capable of performing well.

For white noise base acceleration, it has been shown that the power harvested is proportional to the oscillating mass and the noise intensity and independent of the system used to dissipate it. This result has been partially shown or derived for simple or specific systems in a number of ways [10,11,14–16], but the most general and complete proof is that of [8], extended in [9]. Here it is shown that for an arbitrary degree of freedom system with general nonlinearity dependent on displacement and velocity and excited by stationary white noise base acceleration, the power input, P, from the base excitation is

$$P = \frac{\pi S_0 M_{\mathrm{Tot}}}{2} \tag{1}$$

where S_0 is the single-sided spectral density of the excitation and M_{Tot} is the total oscillating mass. This result is independent of the form of the transduction mechanism and when an electrical circuit is present, the power will be split between electrical and mechanical dissipation. A tighter upper bound more specifically for electrical power dissipation is derived in [16] where a typical harvester circuit is coupled to the mechanical oscillator and it is found that a low frequency device increases the power bound.

White noise is an idealisation of realistic noise and is a valid approximation when the bandwidth of the oscillator is significantly narrower than the bandwidth of the noise. It has been shown in [9] that for a wide class of systems, those that exhibit detailed balance, the power calculated using Eq. (1) will be greater than or equal to the power dissipated under non-white excitation where the peak of the spectrum is taken as S_0. The power from white noise excitation can therefore be thought of as an upper bound for these types of systems, which include a single-degree-of-freedom system with a linear dissipation mechanism.

Many studies into optimal systems for harvesting white noise excitations have been undertaken, for example [11–15,17–19], often with a particular focus on the potential of nonlinear systems to improve power transfer. In general, the best system depends on the model of the electrical circuit; if only a dissipative component is used, the power can be simply found from the ratio of mechanical to equivalent electrical damping and is independent of stiffness nonlinearity. However, in reality the electrical system is more complex than containing a simply dissipative component, with piezoelectric and electrostatic circuits containing a capacitor and electromagnetic ones containing an inductor. With these included, it is found that the stiffness potential used will affect the power output. Furthermore, a number of studies, particularly experimental ones, use non-white excitation with a variety of spectra [11,12,20–23,32,25–27] and generally find that the power output depends more strongly on the type of noise and system investigated.

One type of design of great interest in the literature for both harmonic and broadband excitation is the bistable system [12,18,20,21,25,33–37]. It has been concluded both theoretically and experimentally that these systems improve power generation under broadband random excitation when an appropriate electrical circuit is used, although the exact form of the stiffness profile must be tuned to the excitation level in order to achieve inter-well dynamics. This paper agrees with these results and illustrates how it is that these devices approach maximum power when compared to monostable alternatives.

The aim of this paper is to derive an upper bound on the power available to harvest from white noise excitation. Differently from the common approach of optimising a chosen stiffness profile, the bound encompasses all stiffness nonlinearities and as such allows for easy comparison between the diverse range of energy harvesters and illuminates what characteristics in a harvesting system are required to provide maximum power. In what follows, Section 2 derives the power bound, Section 3 uses numerical simulations of a number of popular devices and compares them to the power bound of Section 2 and finally, Section 4 discusses desirable characteristics of optimal harvesters.

2. An upper bound on power harvested

The present analysis is concerned with a single-degree-of-freedom energy harvester as shown in Fig. 1 which consists of a mass, m, that is connected to a vibratory surface via a linear damper of rate b and a nonlinear spring with restoring force $g(x)$, where x represents the displacement of the mass in relation to the vibrating base. An electrical circuit is coupled to the mass consisting of a capacitor of capacitance C and a nonlinear resistor such that the governing equations are

$$m\ddot{x} + b\dot{x} + g(x) + \theta V = -m\ddot{\xi}(t) \tag{2}$$

$$C\dot{V} + \frac{f(V)}{\gamma} = \theta\dot{x} \tag{3}$$

where θ is the electrical coupling coefficient, V is the voltage over the nonlinear resistor and γ is the nonlinear resistance such that $f(V)/\gamma$ is the current flowing through the resistor. $\ddot{\xi}(t)$ represents the white noise base acceleration with autocorrelation function at a time lag τ of $\pi S_0\delta(\tau)$ where S_0 is the single-sided spectral density and $\delta(\tau)$ is the delta function.

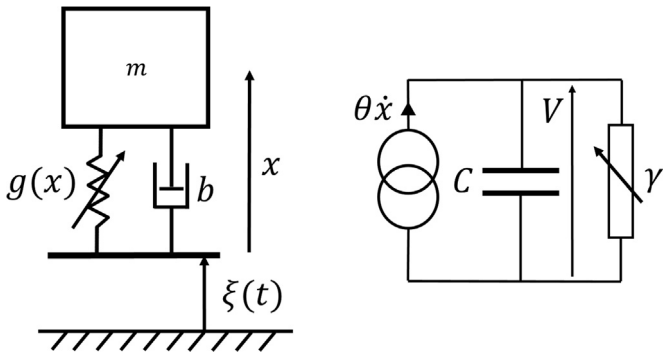

Fig. 1. Model of the energy harvester system with the mechanical oscillator and electrical harvesting circuit.

The harvester includes both a nonlinear spring and nonlinear resistor in order to encompass a broad range of possible harvesting devices. The capacitor in the circuit is typical in piezoelectric energy harvesting systems due to the properties of piezoelectric materials [38]. However, this system could also represent some electrostatic harvesters [27] or electromagnetic harvesters where voltage is exchanged for current and the capacitance becomes the coil inductance of the electromagnet [39]. The nonlinear resistor must be purely dissipative therefore $\text{sign}[f(V)] = \text{sign}[V]$. Eq. (3) will not account for all possible circuits as the nonlinearity of the resistor cannot represent effects from time derivatives or integrals of voltage due to components such as additional capacitors or inductors. However, it will encompass a wider range of circuitry than the commonly assumed linear resistor and will help to assess whether nonlinear resistance profiles provide improved harvesting performance.

It is known from [8] that the power input to the system governed by Eqs. (2) and (3) is equal to $\pi S_0 m/2$ regardless of the specific system properties. This input power will be split between the desired electrical power, P_E, and the undesired mechanical damping, P_M, as follows

$$\frac{\pi S_0 m}{2} = P_M + P_E \tag{4}$$

where

$$P_M = b\mathrm{E}\left[\dot{x}^2\right] \tag{5}$$

$$P_E = \theta\mathrm{E}\left[\dot{x}V\right] \tag{6}$$

and $\mathrm{E}[Z]$ represents the ensemble average of the random variable Z. An alternative expression for the electrical power, P_E, can be obtained by multiplying Eq. (3) by V and taking the ensemble average of the resulting equation. Noting that $\mathrm{E}\left[V\dot{V}\right] = 0$ because the system response is stationary then yields

$$P_E = \frac{\mathrm{E}\left[Vf(V)\right]}{\gamma}. \tag{7}$$

Two upper bounds on the electrical power harvested, P_{EU1} and P_{EU2}, will now be calculated by manipulation of the equations of motion. Both upper bounds are required since one bound is found to limit electrical power dissipation for small γ and the other for large γ. However, at an optimal intermediate value of γ where the two bounds are equal, the maximum upper bound on electrical power is found.

The first bound, P_{EU1}, can be found from calculating the mean square velocity by squaring Eq. (3) and taking the ensemble average to yield

$$\mathrm{E}\left[\dot{x}^2\right] = \frac{1}{\theta^2}\mathrm{E}\left[\left(C\dot{V} + \frac{f(V)}{\gamma}\right)^2\right] \tag{8}$$

$$= \frac{C^2}{\theta^2}\mathrm{E}\left[\dot{V}^2\right] + \frac{2C}{\theta^2\gamma}\mathrm{E}\left[\dot{V}f(V)\right] + \frac{1}{\theta^2\gamma^2}\mathrm{E}\left[f(V)^2\right]. \tag{9}$$

The term $\mathrm{E}\left[\dot{V}f(V)\right]$ that appears in this equation is zero, since the response is stationary meaning that $\mathrm{E}\left[\dot{V}f(V)\right] = \frac{\mathrm{d}}{\mathrm{d}t}\mathrm{E}\left[r(V)\right] = 0$ where $r(V) = \int f(V)\mathrm{d}V$.

Eqs. (4), (5), (7) and (9) can be combined to produce

$$\frac{\pi S_0 m}{2} = \frac{bC^2}{\theta^2}\mathrm{E}\left[\dot{V}^2\right] + \frac{b}{\theta^2\gamma^2}\mathrm{E}\left[f(V)^2\right] + \frac{1}{\gamma}\mathrm{E}\left[Vf(V)\right]. \tag{10}$$

From Eq. (7) the last term on the right hand side represents electrical power dissipation, for which an upper bound, P_{EU1}, is sought. Since maximum electrical power will occur when $\mathrm{E}\left[\dot{V}^2\right]$ is a minimum, an upper bound on power can be given by setting $\mathrm{E}\left[\dot{V}^2\right] = 0$ (which also highlights that when designing a device for maximum electrical power, $\mathrm{E}\left[\dot{V}^2\right]$ must be minimised). This leads to the bound

$$P_{EU1} = \frac{\pi S_0 m}{2} - \frac{b}{\theta^2\gamma^2}\mathrm{E}\left[f(V)^2\right]. \tag{11}$$

A second upper bound on the electrical power, P_{EU2}, can be found by multiplying Eq. (2) by x and taking the ensemble average to give

$$m\mathrm{E}\left[x\ddot{x}\right] + b\mathrm{E}\left[x\dot{x}\right] + \mathrm{E}\left[xg(x)\right] + \theta\mathrm{E}\left[xV\right] = -m\mathrm{E}\left[x\ddot{\xi}\right]. \tag{12}$$

Since the response is stationary, by taking the time derivative of $\mathrm{E}\left[x\dot{x}\right]$ and $\mathrm{E}\left[x^2\right]$ it is found that $\mathrm{E}\left[x\ddot{x}\right] = -\mathrm{E}\left[\dot{x}^2\right]$ and $\mathrm{E}\left[x\dot{x}\right] = 0$. Additionally, $\mathrm{E}\left[x\ddot{\xi}\right] = 0$ since the displacement response at any time cannot be correlated to the excitation at that time for white noise or alternatively, the excitation does not instantaneously affect the displacement. The term $\mathrm{E}\left[xV\right]$ can be assessed by taking the ensemble average of the time integral form of Eq. (3) multiplied by V to yield

$$C\mathrm{E}\left[V^2\right] + \frac{1}{\gamma}\mathrm{E}\left[V\int f(V)\mathrm{d}t\right] = \theta\mathrm{E}\left[xV\right]. \tag{13}$$

The stationary response means that $\frac{\mathrm{d}}{\mathrm{d}t}\mathrm{E}\left[\int V\mathrm{d}t\int f(V)\mathrm{d}t\right] = 0$ and therefore $\mathrm{E}\left[V\int f(V)\mathrm{d}t\right] = -\mathrm{E}\left[\int V\mathrm{d}t f(V)\right]$. If $g(x)$ and $f(V)$ are odd functions, the system is symmetric meaning that the joint probability density function of voltage and its integral, $p\left(\int V\mathrm{d}t, V\right)$, is even in both $\int V\mathrm{d}t$ and V and therefore $\mathrm{E}\left[V\int f(V)\mathrm{d}t\right] = -\mathrm{E}\left[\int V\mathrm{d}t f(V)\right] = 0$. In order to proceed with the upper bound for the electrical power, the restriction that $g(x)$ and $f(V)$ are odd functions must be applied although it is possible that even without this restriction, the term $\mathrm{E}\left[V\int f(V)\mathrm{d}t\right]$ is still equal to zero.

Eqs. (12) and (13) can be combined to yield

$$-m\mathrm{E}\left[\dot{x}^2\right] + \mathrm{E}\left[xg(x)\right] + C\mathrm{E}\left[V^2\right] = 0 \tag{14}$$

where it can be noted that the removal of the electrical term produces the Virial theorem which equates the average value of two times the kinetic energy with the average force multiplied by displacement [40]. Eqs. (4), (5) and (7) can be combined with Eq. (14) giving

$$\frac{\pi S_0 m}{2} = \frac{b}{m}\left(\mathrm{E}\left[xg(x)\right] + C\mathrm{E}\left[V^2\right]\right) + \frac{1}{\gamma}\mathrm{E}\left[Vf(V)\right]. \tag{15}$$

Similar to Eq. (10), the rightmost term represents electrical power and so the second upper bound on the electrical power, P_{EU2}, can be found by applying lower bounds of the terms $\mathrm{E}\left[xg(x)\right]$ and $\mathrm{E}\left[V^2\right]$. The term $\mathrm{E}\left[V^2\right]$ is closely related to the electrical power term via the voltage probability density function (PDF), whereas a lower bound for the term $\mathrm{E}\left[xg(x)\right]$ can be found.

It is clear that for a monostable system, with the origin at the equilibrium point, $xg(x)$ can only be positive therefore $\mathrm{E}\left[xg(x)\right] > 0$. However, for a system with more than one equilibrium position negative regions of $xg(x)$ occur on either one or both sides of an unstable equilibrium point giving the possibility of negative $\mathrm{E}\left[xg(x)\right]$. A simple argument for the positivity of this term can be made by considering equivalent linearisation [41] whereby the nonlinear mechanical stiffness is represented by a linear system of stiffness k_{eq} that minimises the mean square error between the nonlinear and equivalent linear systems. In this case $k_{eq} = \mathrm{E}\left[xg(x)\right]/\mathrm{E}\left[x^2\right]$ and since a positive stiffness must best fit the stable system, $\mathrm{E}\left[xg(x)\right] \geq 0$ thus a minimum of $\mathrm{E}\left[xg(x)\right] = 0$ can be used in Eq. (15) to provide the upper bound for the electrical power.

It cannot be proven using the equations of motion Eqs. (2) and (3) that $\mathrm{E}\left[xg(x)\right] \geq 0$ since a counter-example can be found where $\gamma = \infty$ so the capacitor acts in the mechanical circuit like an extra spring. In this case the spring of the capacitor could stabilise the system about an unstable equilibrium position with a region of negative $xg(x)$, and therefore produce $\mathrm{E}\left[xg(x)\right] < 0$. However, under realistic conditions with finite resistance when $\gamma \neq \infty$ the capacitor is in parallel with a dissipative term so the mechanical system cannot be stabilised by the electrical circuit about an unstable equilibrium position therefore the equivalent linearisation argument above can be applied. This leads to the bound

$$P_{EU2} = \frac{\pi S_0 m}{2} - \frac{bC}{m}\mathrm{E}\left[V^2\right]. \tag{16}$$

Whilst it seems reasonable to assume $\mathrm{E}\left[xg(x)\right] \geq 0$, it has not been formally proven, hence must be classed as an assumption required for the following bound to hold.

In summary two equations have been derived, Eqs. (11) and (16), that provide two upper bounds for the electrical power: P_{EU1} and P_{EU2} respectively. Each equation can be written as an inequality in terms of voltage moments by using Eq. (7) to substitute for the power term, for example Eq. (16) becomes

$$\frac{\mathrm{E}\left[Vf(V)\right]}{\gamma} \leq \frac{\pi S_0 m}{2} - \frac{bC}{m}\mathrm{E}\left[V^2\right]. \tag{17}$$

For the upper bound on power, the limiting case of the inequality must be taken such that the sum of the two terms involving the voltage moments equals $\pi S_0 m/2$ with the relative contributions of each term depending on the PDF of the voltage. An optimal PDF can be hypothesised that both satisfies the limiting case of Eq. (17) (or its equivalent from Eq. (11)) and maximises the contribution of the power term, $\mathrm{E}\left[Vf(V)\right]/\gamma$, consequently minimising the contribution of the other voltage moment term. This requires finding a voltage PDF that maximises $\mathrm{E}\left[Vf(V)\right]$ for a given $\mathrm{E}\left[f(V)^2\right]$ or $\mathrm{E}\left[V^2\right]$ for Eq. (11) or (16) respectively in order to maximise P_{EU1} or P_{EU2} and provide the upper bound.

The aim of this paper is to find the maximum power achievable and it is clear from the bounds in Eqs. (11) and (16) that this will occur when b and C are minimised and m and θ are maximised. However, the optimal value of γ is less apparent. From a superficial analysis of the two bound equations at low and high γ, it is apparent that P_{EU1} increases with γ from zero to $\pi S_0 m/2$ whereas P_{EU2} decreases with γ from $\pi S_0 m/2$ to zero. If both of the power bounds can be shown to vary monotonically with γ, the maximum upper bound on electrical power, P_{Max}, will be achieved when the two bounds cross such that $P_{EU1} = P_{EU2}$ with corresponding optimal γ value, γ_{opt}. The monotonic nature of the bounds is assessed in the appendix and herein P_{EU1} will be assumed to increase and P_{EU2} will be assumed to decrease monotonically with γ.

At the point where the two bounds meet the voltage PDF must be the same for both P_{EU1} and P_{EU2}, although it is not obvious what PDF will maximise power; it could be one that maximises $\mathrm{E}\left[Vf(V)\right]$ for either a given $\mathrm{E}\left[f(V)^2\right]$ or $\mathrm{E}\left[V^2\right]$ or a different distribution. To illustrate this, suppose $f(V) = V^3$ so to maximise P_{EU1} requires maximisation of $\mathrm{E}\left[V^4\right]$ for a given $\mathrm{E}\left[V^6\right]$ therefore a platykurtic voltage distribution with low tail probability. Whereas to maximise P_{EU2} requires maximisation of $\mathrm{E}\left[V^4\right]$ for a given $\mathrm{E}\left[V^2\right]$ therefore a leptokurtic voltage distribution with high tail probability. Whether the maximum power point where $P_{EU1} = P_{EU2}$ is greater for a platykurtic or leptokurtic distribution is not clear and will be found for the general nonlinearity, $f(V)$, in what follows. Examples of a platykurtic and a leptokurtic distribution are compared with a Gaussian distribution all with the same mean square value in Fig. 2.

For the maximum upper bound on electrical power $P_{EU1} = P_{EU2} = P_{\mathrm{Max}}$ and so Eqs. (11) and (16) are equated to provide optimal γ,

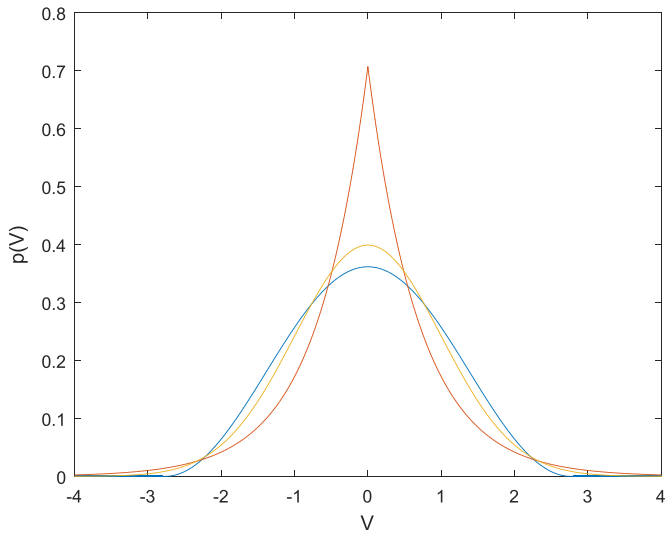

Fig. 2. Probability density functions of a platykurtic (blue), leptokurtic (red) and Gaussian (yellow) system all with the same mean square values.

$$\gamma_{\text{opt}} = \sqrt{\frac{m}{C\theta^2}\frac{\mathrm{E}\left[f(V)^2\right]}{\mathrm{E}\left[V^2\right]}} \tag{18}$$

and therefore using Eq. (7)

$$P_{\text{Max}} = \frac{\mathrm{E}\left[Vf(V)\right]}{\gamma_{\text{opt}}} \tag{19}$$

$$= \sqrt{\frac{C\theta^2}{m}\frac{\mathrm{E}\left[V^2\right]}{\mathrm{E}\left[f(V)^2\right]}}\,\mathrm{E}\left[Vf(V)\right]. \tag{20}$$

Eq. (20) can be rearranged to give $\mathrm{E}\left[V^2\right]$ in terms of P_{Max} and the voltage moments

$$\mathrm{E}\left[V^2\right] = P_{\text{Max}}\sqrt{\frac{m}{C\theta^2}}\frac{\sqrt{\mathrm{E}\left[f(V)^2\right]\mathrm{E}\left[V^2\right]}}{\mathrm{E}\left[Vf(V)\right]} \tag{21}$$

which can be substituted into Eq. (16) with $P_{EU2} = P_{\text{Max}}$ yielding

$$\frac{\pi S_0 m}{2} = P_{\text{Max}}\left(\sqrt{\frac{b^2C}{\theta^2 m}}\frac{\sqrt{\mathrm{E}\left[f(V)^2\right]\mathrm{E}\left[V^2\right]}}{\mathrm{E}\left[Vf(V)\right]} + 1\right). \tag{22}$$

Clearly the voltage PDF that minimises $\sqrt{\mathrm{E}\left[f(V)^2\right]\mathrm{E}\left[V^2\right]}/\mathrm{E}\left[Vf(V)\right]$ provides the maximum value of P_{Max}. The minimum of this term is demonstrated to be unity as follows. The positive definite integral below provides an initial inequality

$$\int_{-\infty}^{\infty}\int_{-\infty}^{\infty}\left[V_2 f(V_1) - V_1 f(V_2)\right]^2 p(V_1)p(V_2)\mathrm{d}V_1\mathrm{d}V_2 \geq 0 \tag{23}$$

that can be rearranged to yield

$$\int_{-\infty}^{\infty}\int_{-\infty}^{\infty}\left[V_2^2 f(V_1)^2 + V_1^2 f(V_2)^2 - 2V_1V_2 f(V_1)f(V_2)\right]p(V_1)p(V_2)\mathrm{d}V_1\mathrm{d}V_2 \geq 0 \tag{24}$$

$$p(V_1)p(V_2)\mathrm{d}V_1\mathrm{d}V_2 \geq 0 \tag{25}$$

$$2\mathrm{E}\left[V^2\right]\mathrm{E}\left[f(V)^2\right] - 2\mathrm{E}\left[Vf(V)\right]^2 \geq 0 \tag{26}$$

$$\mathrm{E}\left[V^2\right]\mathrm{E}\left[f(V)^2\right] \geq \mathrm{E}\left[Vf(V)\right]^2 \tag{27}$$

$$\frac{\sqrt{\mathrm{E}\left[f(V)^2\right]\mathrm{E}\left[V^2\right]}}{\mathrm{E}\left[Vf(V)\right]} \geq 1. \tag{28}$$

The PDF, $p(V)$, that provides the limiting case of the inequality is the most extreme platykurtic distribution taking the form of two delta functions at $\pm V_k$

$$p(V) = \frac{1}{2}\delta(V - V_k) + \frac{1}{2}\delta(V + V_k) \tag{29}$$

where V_K is an arbitrary positive voltage. Any moments required in Eq. (28) are even functions of V since $f(V)$ is an odd function therefore with the PDF of Eq. (29) and any even function, $h(V)$, the ensemble average of $h(V)$ is

$$\mathrm{E}\left[h(V)\right] = \int_{-\infty}^{\infty} h(V)p(V)\mathrm{d}V = h(V_k) \tag{30}$$

and so

$$\frac{\sqrt{\mathrm{E}\left[f(V)^2\right]\mathrm{E}\left[V^2\right]}}{\mathrm{E}\left[Vf(V)\right]} = 1. \tag{31}$$

Alternatively, a linear resistor, where $f(V) = V$, provides this result regardless of the voltage PDF. Substituting this maximum power case from Eq. (31) into Eq. (22) provides an upper bound on power available to harvest

$$P_{\text{Max}} = \frac{\sqrt{\theta^2 m}}{\sqrt{b^2C} + \sqrt{\theta^2 m}}\frac{\pi S_0 m}{2}. \tag{32}$$

3. Examples

Three examples will now be used to illustrate the upper bound of Eq. (32) and compare a number of common harvesters to it.

3.1. Example 1: linear resistance and stiffness

A useful starting point is provided by analysis of a purely linear system. Substituting $g(x) = kx$, $f(V) = V$ and $\gamma = R$ which represents linear electrical resistance into the equations of motion, Eqs. (2) and (3), the electrical power harvested can be found analytically as

$$P_E = \frac{m\theta^2 R}{bkC^2R^2 + b^2CR + bC\theta^2R^2 + bm + m\theta^2 R}\frac{\pi S_0 m}{2}. \tag{33}$$

From Eq. (33), maximum power is harvested when the linear stiffness is zero and an optimal resistance can then be found by differentiation as $R = \sqrt{m/C\theta^2}$. With these values, the maximum power harvested by a purely linear harvester, P_{EMaxLin}, can be found to be

$$P_{\mathrm{EMaxLin}} = \frac{m\theta^2}{\left(\sqrt{b^2C} + \sqrt{\theta^2 m}\right)^2}\frac{\pi S_0 m}{2} \tag{34}$$

and compared to the upper bound of Eq. (32). Both equations multiply the total power input by the white noise from Eq. (4) by a term less than unity, but the multiplying term for the optimal linear system is the square of that of the power bound and therefore always smaller than the bound. The result is that when the contribution of the linear damping and capacitance is large compared with the contribution of the electromechanical coupling factor and the mass, the upper bound of Eq. (32) provides a loose bound far from the power of the real linear device. Conversely, when the contribution of the linear damping and capacitance is small compared with the contribution of the electromechanical coupling factor and the mass the power from the linear system is close to its upper limit and hence no other system will be able to significantly outperform a linear one.

3.2. Example 2: linear resistance, nonlinear stiffness

A frequently analysed energy harvester in the literature [39,38,21] is one with a linear resistance, R, and nonlinear mechanical restoring force. Putting $\gamma = R$ and $f(V) = V$ in Eq. (3) yields

$$C\dot{V} + \frac{V}{R} = \theta\dot{x}. \tag{35}$$

Using this equation of motion with Eq. (2) and noting $\mathrm{E}\left[f(V)^2\right] = \mathrm{E}\left[Vf(V)\right] = \mathrm{E}\left[V^2\right]$ in Eqs. (11) and (16) the bounds become

$$P_{EU1} = \frac{R\theta^2}{b + R\theta^2}\frac{\pi S_0 m}{2} \tag{36}$$

$$P_{EU2} = \frac{m}{m + bCR}\frac{\pi S_0 m}{2}. \tag{37}$$

These two bounds are equal and provide the maximum of Eq. (32) when $R = \sqrt{m/C\theta^2}$. Interpreting the expressions of Eqs. (36) and (37) physically reveals that the first shows the system is like a potential divider between mechanical damping and equivalent electrical damping, $R\theta^2$, from the resistor. As the electrical damping increases, more of the input power, $\pi S_0 m/2$, is dissipated electrically rather than mechanically. The second bound is less apparent, but shows that if the time constant, CR, of the electrical circuit is too large then less energy will be able to flow into the electrical circuit so less power will be dissipated in it.

In order to assess how prominent devices compare to the power bounds, a number of popular stiffness profiles have been simulated to calculate their power under white noise excitation. The optimal linear device has been found in Example 1 to be one with zero stiffness, $g(x) = 0$ N, and this is compared to the Duffing oscillator of the form $g(x) = k_1x + k_3x^3$ in a monostable configuration ($k_1 = 100\ \mathrm{N\ m^{-1}}$ and $k_3 = 2 \times 10^9\ \mathrm{N\ m^{-3}}$) and a bistable configuration ($k_1 = -40\ \mathrm{N\ m^{-1}}$ and $k_3 = 3 \times 10^9\ \mathrm{N\ m^{-3}}$) that was tuned to produce maximum power at optimal resistance. Additionally, a device with linear stiffness ($k_1 = 10\ \mathrm{N\ m^{-1}}$ and $k_3 = 0\ \mathrm{N\ m^{-3}}$), but with end stops restricting motion of a mass was also compared. The comparison is presented in Fig. 3 where power is plotted against resistance and all simulations are found to lie beneath the power bounds of Eqs. (32), (36) and (37). Parameter values representative of a small energy harvester are used with $m = 1 \times 10^{-3}$ kg, $b = 5 \times 10^{-3}\ \mathrm{N\ s\ m^{-1}}$, $\theta = 1 \times 10^{-4}\ \mathrm{N\ V^{-1}}$, $S_0 = (2 \times 10^{-3}/\pi)\ \mathrm{m^2\ s^{-3}}$ and $C = 1 \times 10^{-9}$ F.

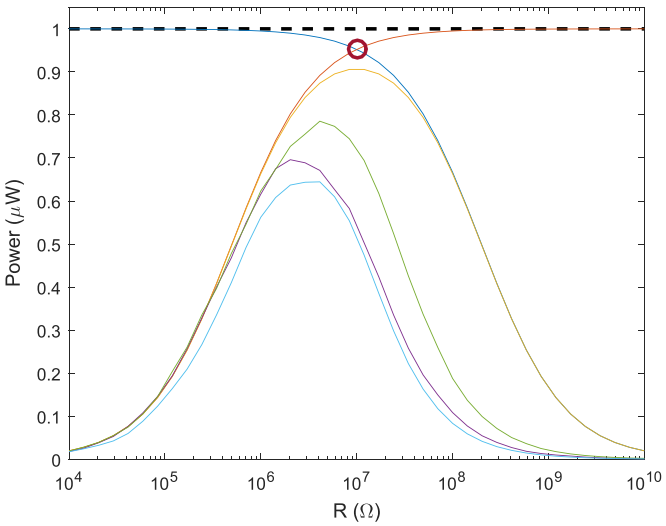

Fig. 3. Comparison of a number of harvesting systems to the power bounds with linear electrical resistance. $\pi S_0 m/2$ (black dashes), Eq. (36) (red), Eq. (37) (dark blue), Eq. (32) (red circle), zero stiffness (yellow), Duffing (purple), bistable (green) and end stops (light blue).

3.3. *Example 3: cubic resistance asymmetric nonlinear stiffness*

In some circumstances nonlinear electrical components can be used to attempt to improve power dissipation or maintain performance whilst improving another characteristic such as reducing the displacement of the device. To illustrate this, three systems were simulated: one with zero stiffness, $g(x) = 0$ N, one with a symmetric bistable potential ($k_1 = -40$ N m^{-1} and $k_3 = 6 \times 10^{10}$ N m^{-3}) and one with an asymmetric bistable potential where $g(x) = k_1x + k_2x^2 + k_3x^3$ with $k_1 = -40$ N m^{-1}, $k_2 = 10^6$ N m^{-2} and $k_3 = 6 \times 10^{10}$ N m^{-3}, all coupled to a cubic nonlinear resistance where $f(V) = V^3$. All other parameters were the same as in Example 2.

Applying this nonlinear resistance to the bounds of Eqs. (11) and (16) reveals that for maximum power according to Eq. (11) the most extreme platykurtic distribution of Eq. (29) is desired and so Eq. (11) can be solved for V_k and therefore P_{EU1}. Whereas for an upper bound on power, Eq. (16) requires the most extreme leptokurtic distribution for which there is no upper bound. To illustrate the curve of Eq. (16), a conservative estimate using a Laplace distribution of voltage (as seen in Fig. 2) where $\mathrm{E}\left[V^4\right]/\mathrm{E}\left[V^2\right]^2 = 6$ has been used. However, this is no longer an upper bound curve since more power could be dissipated if a voltage distribution of higher kurtosis could be attained.

The power bounds and the power harvested from the selected devices are plotted against γ in Fig. 4. Again, the systems are seen to perform within the power bound of Eq. (11) and below the conservative estimate of Eq. (16) when using a Laplace distribution for voltage. Consequently, no system is found to surpass the maximum available power of Eq. (32). Again, the zero stiffness device performs best, but not as close to the bounds for linear resistance. Additionally, the asymmetric bistable system is included in the plot to illustrate that whilst the bounds do not apply to asymmetric systems, it is improbable that asymmetry will significantly improve performance.

The curve from Eq. (16) is also plotted with the voltage distribution of Eq. (29) to show that under this condition, the two lines of Eqs. (11) and (16) cross at the maximum power point of Eq. (32) shown by the dashed purple line. Clearly the zero stiffness oscillator has a more leptokurtic voltage distribution for high γ therefore provides more power than when the voltage distribution of Eq. (29) is used. However, the Laplace distribution seems to be a good upper bound estimate.

4. Optimal device design

The designer of an energy harvester will want to both select parameters that maximise the power bound of Eq. (32) and then create a device whose performance approaches it. In terms of optimal system parameters, Eq. (32) shows that maximising the oscillating mass and electrical coupling and removal of both mechanical damping and the capacitance (or coil resistance in an electromagnetic harvester) will increase the maximum power available. The majority of these parameters will be restricted by design or material constraints, therefore it is essential to select the optimal resistance (or nonlinear equivalent).

In order to design a device that approaches the bound, a summary of the conditions necessary for a harvester to achieve this bound is useful. In general, these conditions will be impossible to achieve, but if a device can be designed for which

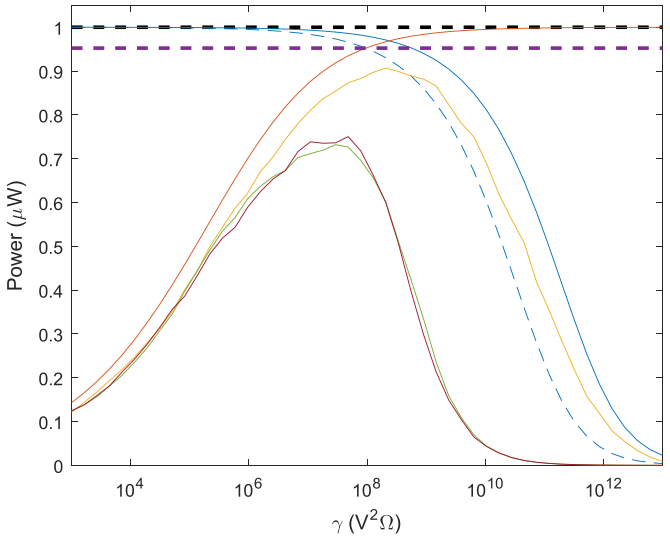

Fig. 4. Comparison of a number of harvesting systems to the power bounds with cubic electrical resistance. $\pi S_0 m/2$ (black dashes), Eq. (11) (red), Eq. (16) with Laplace distribution where $\mathrm{E}\left[V^4\right]/\mathrm{E}\left[V^2\right]^2 = 6$ (solid dark blue), Eq. (16) with distribution of Eq. (29) where $\mathrm{E}\left[V^4\right]/\mathrm{E}\left[V^2\right]^2 = 1$ (dashed dark blue), zero stiffness (yellow), bistable (green), asymmetric bistable (maroon) and Eq. (32) (purple dashes).

these conditions can be approached then a harvester will perform close to the upper bound. Firstly the lower limit of $\mathrm{E}\left[\dot{V}^2\right] = 0$ should be examined alongside the requirement to maximise the power $\mathrm{E}\left[Vf(V)\right]$. Together, these suggest that a low frequency voltage response is desired; a result that is unsurprising considering the electrical circuit acts like a low-pass filter. This agrees well with [16] where a low frequency response also provides an increased power bound.

Secondly, assuming that $\mathrm{E}\left[xg(x)\right] \geq 0$, how to achieve the lower limit is not obvious. When no electrical coupling is present $\mathrm{E}\left[xg(x)\right] = \pi S_0 m^2/2b$ regardless of $g(x)$ therefore the optimal stiffness profile is one that decreases $\mathrm{E}\left[xg(x)\right]$ most significantly when electrical coupling is applied. For many systems $xg(x)$ will increase with $|x|$, therefore minimising $\mathrm{E}\left[xg(x)\right]$ is equivalent to requiring the electrical circuit to decrease the amplitude of the motion as much as possible. From the equivalent linearisation argument made earlier this should also be true for systems where $xg(x)$ does not increase with $|x|$. In keeping with the minimisation of $\mathrm{E}\left[\dot{V}^2\right]$ and since the impedance of the capacitor is high at low frequencies, the circuit will reduce the displacement most for a low frequency response.

Additionally, when a nonlinear resistor is used, the voltage PDF of Eq. (29) is required to achieve the maximum power of Eq. (32). This is clearly unrealistic although it emphasises that the most platykurtic voltage distribution achievable is desired. This could be sought through a combination of stiffness and electrical nonlinearities. However, for the case of linear resistance the maximum power is not dependent on the voltage distribution therefore linear electronics may be a useful method for bypassing this assumption.

In summary, the most important property for a harvester aiming to approach the upper bound on power is a low frequency response. This ensures both $\mathrm{E}\left[\dot{V}^2\right]$ and $\mathrm{E}\left[xg(x)\right]$ are low and provided the resistance is linear, the voltage distribution is unimportant. A low frequency response will typically be enabled by a low stiffness device, hence the zero stiffness system in Figs. 3 and 4 performs close to the bound. If a lower frequency device could be devised, it is assumed that its performance could be improved further.

In practice, zero stiffness is not possible since it would require infinite displacement. However, low stiffness devices with finite displacement are achievable. A bistable device is a good example where, if well tuned for inter-well dynamics, the majority of the oscillations will occur within a displacement range of relatively low potential, or a low stiffness region, yet it still has a high stiffness at large displacement to restrict motion.

A useful property of this power bound is that it encompasses both linear and nonlinear stiffness profiles and can therefore provide some insight into the pertinent question of whether nonlinear devices perform better than linear ones. Whilst no device will be able to surpass the bound, it is not known whether a nonlinearity can enable a device to come closest to the bound. Given the requirement of a low stiffness device it seems a zero stiffness (linear) device is optimal, but not possible due to practical considerations. A nonlinear device like a bistable one therefore becomes attractive as it provides low stiffness for maximum power, but also restricts displacement and is physically realisable.

In the examples above, the nonlinear resistance has not provided an increase in maximum power (achieved with zero stiffness) since with the linear and cubic resistances the maximum power was found to be 0.91 μW for both. It may be

possible that other electrical nonlinearities improve performance, although since power close to the bound can be achieved by simply using a linear resistance unless there is a practical reason to use a nonlinear resistance, the improvement may not be worth the increased complexity.

5. Conclusions

A new upper bound on harvested power has been derived for a single-degree-of-freedom harvester under white noise base excitation with a general stiffness nonlinearity and coupled to a nonlinear electrical circuit. The bound could not be proven for the most general case and therefore a number of limitations exist meaning the bound is only valid if:

- The harvester contains a single oscillating mass with linear mechanical damping and equations of motion in the form of Eqs. (2) and (3). This is typical of the majority of common harvester designs.
- The voltage moment term $\mathrm{E}\left[V\int f(V)\mathrm{d}t\right]$ is equal to zero. This is true if the system is symmetric, meaning $g(x)$ and $f(x)$ in Eqs. (2) and (3) are odd functions.
- The inequality $\mathrm{E}\left[xg(x)\right]\geq 0$ is true. This is certainly true for monostable systems and assumed to be true from an equivalent linearisation argument for systems with more than one equilibrium point.
- The upper bounds of Eqs. (11) and (16) are equal at only one value of nonlinear resistance and this point gives an upper bound on electrical power. This is true if the bounds vary monotonically with γ which has been shown to be the case when $f(V)$ is monotonically increasing and the inequality of Eq. (A.12) is satisfied.

The latter three conditions each yield classes of systems for which the condition is definitely met. However, if a system is devised that is not in one of these classes, it may still satisfy the relevant condition and thus be bound by the upper limit of Eq. (32). For example, a system with more than one equilibrium point, may still satisfy the condition that $\mathrm{E}\left[xg(x)\right]\geq 0$, although it cannot be rigorously proven mathematically.

The limiting cases that produce the upper bound were used to examine the type of system that can come close to the bound and produce maximum power. It was found that due to the low-pass nature of the circuitry, the lower the mechanical stiffness, the more electrical power produced. A zero linear stiffness device is therefore seen to come closest to the bounds, although it is difficult to achieve in practice due to its large displacement response. A bistable system that possesses a low stiffness region, but with stronger restoring forces at large displacements is therefore thought to be a good design for approaching the power bound although it must be tuned to the level of excitation.

Further work extending the power bound to other excitation conditions such as non-white excitation, nonlinear damping and more general electrical circuitry would improve applicability. However, as it stands it is thought to be a useful upper bound since for linearly damped and therefore the majority of systems white noise is an upper bound on any non-white noise with the same peak spectrum [9]. Additionally, mechanical damping will be minimised and therefore be small compared to electrical damping meaning higher fidelity damping modelling will be unlikely to make a large difference. Furthermore, the use of a purely resistive electrical component (excluding the unavoidable piezoelectric capacitor or electromagnetic inductance) to model the circuit dynamics will likely provide an upper bound on power since more complex circuitry will include greater parasitic losses.

By taking the ratio of power generated by a harvester to its upper bound of Eq. (32), the performance of devices designed for harvesting energy from broadband random vibrations can be compared against each other. Additionally, the bound can be used to provide a quick estimate of the power available to harvest in a given operating environment in order to estimate the required harvester specification and thus the feasibility of vibration harvesting.

Acknowledgements

The authors would like to thank the EPSRC for providing the Doctoral Training Award and Programme Grant "Engineering Nonlinearity" EP/K003836/1 that have funded this research. Additional data related to this publication is available at the University of Cambridge data repository https://doi.org/10.17863/CAM.6934.

Appendix A. Monotonically varying bounds

In this appendix, the variation of the two power bounds of Eqs. (11) and (16) with γ is investigated in order to determine if the variation is monotonic. To solve either equation for a given set of the system parameters, the form of a voltage PDF, $p(V)$, is proposed and then a scaled version of the PDF, $Kp(KV)$, can be substituted into either Eqs. (11) or (16) which provides the required scaling factor, K. As different values of γ are selected, but keeping the same form of the PDF, both the scaling value, K, and the upper bound on power will vary. This appendix investigates under what conditions the change in the upper power bound with γ will be monotonic.

Starting with the simpler of the two bounds, Eq. (16); $\mathrm{E}\left[V^2\right]$ can be called σ^2 and $\mathrm{E}\left[Vf(V)\right]$ can be written as a function of σ^2 such that

$$\mathrm{E}\left[Vf(V)\right] = \alpha(\sigma^2). \tag{A.1}$$

This form of equation is possible because as K varies, any one value of mean square voltage will result in a value for the moment $\mathrm{E}\left[Vf(V)\right]$ thus the two can be related by the function α. Using Eq. (A.1) the change in either upper bound, P_{EU1} or P_{EU2}, with respect to γ is found by differentiation of Eq. (7) by γ yielding

$$\frac{\partial P_{EU1/2}}{\partial \gamma} = -\frac{\alpha(\sigma^2)}{\gamma^2} + \frac{1}{\gamma}\frac{\partial \sigma^2}{\partial \gamma}\frac{\partial \alpha(\sigma^2)}{\partial \sigma^2} \tag{A.2}$$

and similarly differentiation of the right hand side of Eq. (16) provides

$$\frac{\partial P_{EU2}}{\partial \gamma} = -\frac{bC}{m}\frac{\partial \sigma^2}{\partial \gamma}. \tag{A.3}$$

Equating Eqs. (A.2) and (A.3) gives the value of $\frac{\partial \sigma^2}{\partial \gamma}$ which can be substituted back into Eq. (A.3) to provide the change in the bound with γ

$$\frac{\partial P_{EU2}}{\partial \gamma} = -\frac{bC\alpha(\sigma^2)}{m\gamma^2}\frac{1}{\frac{1}{\gamma}\frac{\partial \alpha(\sigma^2)}{\partial \sigma^2} + \frac{bC}{m}}. \tag{A.4}$$

The value of $\frac{\partial \alpha(\sigma^2)}{\partial \sigma^2}$ will be positive definite if the function $f(V)$ is monotonically increasing such that an increase in $\mathrm{E}\left[V^2\right]$ will always provide an increase in $\mathrm{E}\left[Vf(V)\right]$, although it may well be positive for non-monotonic functions of $f(V)$ with certain PDF shapes. In this case the right hand side of Eq. (A.4) will be negative and so P_{EU2} will decrease monotonically with γ.

A similar analysis for P_{EU1} does not prove that P_{EU1} increases monotonically with γ from zero to $\pi S_0 m/2$ for all possible functions $f(V)$ and voltage PDF shapes. However, a criterion can be derived that provides a quick check for whether a given electrical nonlinearity and voltage PDF will provide a monotonic bound. Starting again by defining a function to relate the mean square value of $f(V)$ to the mean square voltage

$$\mathrm{E}\left[f^2(V)\right] = \beta(\sigma^2). \tag{A.5}$$

Differentiation of Eq. (11) with respect to γ and substitution of Eq. (A.5) yields

$$\frac{\partial P_{EU1}}{\partial \gamma} = \frac{2b}{\theta^2\gamma^3}\beta(\sigma^2) - \frac{b}{\theta^2\gamma^2}\frac{\partial \sigma^2}{\partial \gamma}\frac{\partial \beta(\sigma^2)}{\partial \sigma^2}. \tag{A.6}$$

Again, $\frac{\partial \sigma^2}{\partial \gamma}$ can be found by equating Eqs. (A.2) and (A.6) then substituted into Eq. (A.2) to yield

$$\frac{\partial P_{EU1}}{\partial \gamma} = \frac{b}{\gamma^3\theta^2}\frac{1}{\alpha' + \frac{b}{\theta^2\gamma}\beta'}\left(2\beta\alpha' - \alpha\beta'\right) \tag{A.7}$$

where α' and β' represent differentiation with respect to σ^2 and again are both positive if $f(V)$ increases monotonically since the moments of $Vf(V)$ and $f^2(V)$ will both increase as σ^2 increases, but may well be positive for non-monotonic functions of $f(V)$ and certain PDF shapes. The increase in P_{EU1} with γ will be monotonic if

$$2\beta\alpha' - \alpha\beta' > 0. \tag{A.8}$$

Noting that the left hand side of Eq. (A.8) can be rearranged as

$$2\beta\alpha' - \alpha\beta' = \alpha\beta\frac{\partial}{\partial \sigma^2}\left(\ln\left(\frac{\alpha^2}{\beta}\right)\right) \tag{A.9}$$

the inequality will be satisfied if α^2/β, or $\mathrm{E}\left[Vf(V)\right]^2/\mathrm{E}\left[f^2(V)\right]$, always increases as the mean square voltage, σ^2, increases. Whilst it seems likely that this is the case because the numerator is of higher order in V than the denominator, there is no obvious proof and so the condition of Eq. (A.8) is investigated further by substitution of the voltage PDF in the form $Kp(KV)$. A small increase in K, δK will provide a small decrease in σ^2, $\delta\sigma^2$, such that $\frac{\partial K}{\partial \sigma^2} < 0$. Using this PDF in Eq. (A.8) yields

$$2\int f^2(V)Kp(KV)\mathrm{d}V\frac{\partial K}{\partial\sigma^2}\frac{\partial}{\partial K}\left(\int Vf(V)Kp(KV)\mathrm{d}V\right)-\int Vf(V)Kp(KV)\mathrm{d}V\frac{\partial K}{\partial\sigma^2}\frac{\partial}{\partial K}\left(\int f^2(V)Kp(KV)\mathrm{d}V\right)>0. \tag{A.10}$$

Removing the $\frac{\partial K}{\partial\sigma^2}$ terms inverts the inequality and making the substituting $\hat{V}=KV$ provides

$$2\int f^2\left(\frac{\hat{V}}{K}\right)p(\hat{V})\mathrm{d}\hat{V}\frac{\partial}{\partial K}\left(\int\frac{\hat{V}}{K}f\left(\frac{\hat{V}}{K}\right)p(\hat{V})\mathrm{d}\hat{V}\right)-\int\frac{\hat{V}}{K}f\left(\frac{\hat{V}}{K}\right)p(\hat{V})\mathrm{d}\hat{V}\frac{\partial}{\partial K}\left(\int f^2\left(\frac{\hat{V}}{K}\right)p(\hat{V})\mathrm{d}\hat{V}\right)<0. \tag{A.11}$$

Performing the differentiations inside the integrals yields the criterion for monotonically increasing P_{EU1}

$$\mathrm{E}\left[Vf(V)f'(V)\right]\mathrm{E}\left[Vf(V)\right]-\mathrm{E}\left[f^2(V)\right]\left(\mathrm{E}\left[Vf(V)\right]+\mathrm{E}\left[V^2f'(V)\right]\right)<0 \tag{A.12}$$

where $f'(V)=\mathrm{d}f/\mathrm{d}V$. To prove that P_{EU1} always increases monotonically with γ, the criterion of Eq. (A.12) would have to be met for all possible electrical nonlinearities, $f(V)$, and all possible voltage PDFs, $p(V)$. This would require proving exhaustively and so is not investigated here, although two useful cases are shown: when $\mathrm{E}\left[h(V)\right]=h(V_K)$, for any symmetric function $h(V)$ where V_K is an arbitrary positive voltage, and for any power law electrical nonlinearity, $f(V)=AV^n$.

The former case is of interest because this PDF maximises P_{EU1} and provides the bound of Eq. (32). The left hand side of Eq. (A.12) becomes $-f^3(V_K)V_K$ which is less than zero so the bound is monotonic for this PDF. For the case where $f(V)=AV^n$, the left hand side of Eq. (A.12) becomes $-A^3\mathrm{E}\left[V^{n+1}\right]\mathrm{E}\left[V^{2n}\right]$ which is less than zero so the bound is monotonic for this electrical nonlinearity. Whether or not the criterion of Eq. (A.12) is met for other nonlinear functions, $f(V)$, could be assessed computationally by proposing a general form of voltage PDF such as

$$p(V)=B\exp\left(\sum_{n=1}^{N}a_nV^{2n}\right) \tag{A.13}$$

and using an optimisation solver to find values of the a_n coefficients that maximise the left hand side of Eq. (A.12) to see if it can go above zero.

In this paper P_{EU1} and P_{EU2} are assumed to vary monotonically with γ. If $f(V)$ is monotonically increasing, this will be true for P_{EU2} and seems a reasonable assumption for P_{EU1} from the criterion of Eq. (A.12), but for any general electrical nonlinearity this must be assessed against the criterion to ensure that the bounds are monotonic.

References

[1] S.P. Beeby, M.J. Tudor, N.M. White, Energy harvesting vibration sources for microsystems applications, Meas. Sci. Technol. 17 (12) (2006) R175–R195, http://dx.doi.org/10.1088/0957-0233/17/12/R01.
[2] P. Mitcheson, E. Yeatman, G. Rao, A. Holmes, T. Green, Energy harvesting from human and machine motion for wireless electronic devices, Proc. IEEE 96 (9) (2008) 1457–1486, http://dx.doi.org/10.1109/JPROC.2008.927494.
[3] S. Roundy, P.K. Wright, J. Rabaey, A study of low level vibrations as a power source for wireless sensor nodes, Comput. Commun. 26 (11) (2003) 1131–1144, http://dx.doi.org/10.1016/S0140-3664(02)00248-7.
[4] A.R.M. Siddique, S. Mahmud, B.V. Heyst, A comprehensive review on vibration based micro power generators using electromagnetic and piezoelectric transducer mechanisms, Energy Convers. Manag. 106 (2015) 728–747, http://dx.doi.org/10.1016/j.enconman.2015.09.071.
[5] N. Stephen, On energy harvesting from ambient vibration, J. Sound Vib. 293 (1–2) (2006) 409–425, http://dx.doi.org/10.1016/j.jsv.2005.10.003.
[6] J.M. Renno, M.F. Daqaq, D.J. Inman, On the optimal energy harvesting from a vibration source, J. Sound Vib. 320 (1–2) (2009) 386–405, http://dx.doi.org/10.1016/j.jsv.2008.07.029.
[7] R. Ramlan, M.J. Brennan, B.R. Mace, I. Kovacic, Potential benefits of a non-linear stiffness in an energy harvesting device, Nonlinear Dyn. 59 (4) (2010) 545–558, http://dx.doi.org/10.1007/s11071-009-9561-5.
[8] R.S. Langley, A general mass law for broadband energy harvesting, J. Sound Vib. 333 (3) (2014) 927–936, http://dx.doi.org/10.1016/j.jsv.2013.09.036.
[9] R.S. Langley, Bounds on the vibrational energy that can be harvested from random base motion, J. Sound Vib. 339 (2015) 247–261, http://dx.doi.org/10.1016/j.jsv.2014.11.012.
[10] J. Scruggs, An optimal stochastic control theory for distributed energy harvesting networks, J. Sound Vib. 320 (2009) 707–725, http://dx.doi.org/10.1016/j.jsv.2008.09.001.
[11] M.F. Daqaq, Response of uni-modal duffing-type harvesters to random forced excitations, J. Sound Vib. 329 (18) (2010) 3621–3631, http://dx.doi.org/10.1016/j.jsv.2010.04.002.
[12] M.F. Daqaq, Transduction of a bistable inductive generator driven by white and exponentially correlated Gaussian noise, J. Sound Vib. 330 (11) (2011) 2554–2564, http://dx.doi.org/10.1016/j.jsv.2010.12.005.
[13] M.F. Daqaq, On intentional introduction of stiffness nonlinearities for energy harvesting under white Gaussian excitations, Nonlinear Dyn. 69 (3) (2012) 1063–1079, http://dx.doi.org/10.1007/s11071-012-0327-0.
[14] P. Green, K. Worden, K. Atallah, N. Sims, The benefits of Duffing-type nonlinearities and electrical optimisation of a mono-stable energy harvester under white Gaussian excitations, J. Sound Vib. 331 (20) (2012) 4504–4517, http://dx.doi.org/10.1016/j.jsv.2012.04.035.
[15] E. Halvorsen, Energy harvesters driven by broadband random vibrations, J. Microelectromech. Syst. 17 (5) (2008) 1061–1071, http://dx.doi.org/10.1109/JMEMS.2008.928709.
[16] E. Halvorsen, Fundamental issues in nonlinear wideband-vibration energy harvesting, Phys. Rev. E 87 (4) (2013) 042129, http://dx.doi.org/10.1103/PhysRevE.87.042129.
[17] Q. He, M.F. Daqaq, Influence of potential function asymmetries on the performance of nonlinear energy harvesters under white noise, J. Sound Vib. 333 (15) (2014) 3479–3489, http://dx.doi.org/10.1016/j.jsv.2014.03.034.
[18] Q. He, M.F. Daqaq, New insights into utilizing bistability for energy harvesting under white noise, J. Vib. Acoust. 137 (2) (2015) 021009, http://dx.doi.org/10.1115/1.4029008.

[19] H.T. Zhu, Probabilistic solution of a Duffing-type energy harvester system under Gaussian white noise, ASCE-ASME J. Risk Uncert. Eng. Syst. Part B: Mech. Eng., 1, 011005, http://dx.doi.org/10.1115/1.4029143.
[20] F. Cottone, H. Vocca, L. Gammaitoni, Nonlinear energy harvesting, Phys. Rev. Lett. 102 (8) (2009) 080601, http://dx.doi.org/10.1103/PhysRevLett.102.080601.
[21] F. Cottone, L. Gammaitoni, H. Vocca, M. Ferrari, V. Ferrari, Piezoelectric buckled beams for random vibration energy harvesting, Smart Mater. Struct. 21 (3) (2012) 035021, http://dx.doi.org/10.1088/0964-1726/21/3/035021.
[22] L. Gammaitoni, I. Neri, H. Vocca, Nonlinear oscillators for vibration energy harvesting, Appl. Phys. Lett. 94 (16) (2009) 164102, http://dx.doi.org/10.1063/1.3120279.
[23] R.L. Harne, K.W. Wang, Prospects for nonlinear energy harvesting systems designed near the elastic stability limit when driven by colored noise, J. Vib. Acoust. 136 (2) (2014) 021009, http://dx.doi.org/10.1115/1.4026212.
[24] H.K. Joo, T.P. Sapsis, Performance measures for single-degree-of-freedom energy harvesters under stochastic excitation, J. Sound Vib. 333 (19) (2014) 4695–4710, http://dx.doi.org/10.1016/j.jsv.2014.05.003.
[25] D. Meimukhin, N. Cohen, I. Bucher, On the advantage of a bistable energy harvesting oscillator under band-limited stochastic excitation, J. Intell. Mater. Syst. Struct. 24 (14) (2013) 1736–1746, http://dx.doi.org/10.1177/1045389X13484102.
[26] V. Méndez, D. Campos, W. Horsthemke, Efficiency of harvesting energy from colored noise by linear oscillators, Phys. Rev. E 88 (2) (2013) 022124, http://dx.doi.org/10.1103/PhysRevE.88.022124.
[27] S.D. Nguyen, E. Halvorsen, G.U. Jensen, Wideband MEMS energy harvester driven by colored noise, J. Microelectromech. Syst. 22 (4) (2013) 892–900, http://dx.doi.org/10.1109/JMEMS.2013.2248343.
[28] E. Halvorsen, C.P. Le, P.D. Mitcheson, E.M. Yeatman, Architecture-independent power bound for vibration energy harvesters, J. Phys.: Conf. Ser., 476, 2013, 012026, http://dx.doi.org/10.1088/1742-6596/476/1/012026.
[29] J. Heit, S. Roundy, A framework for determining the maximum theoretical power output for a given vibration energy, J. Phys.: Conf. Ser., 557, 2014, 012020, http://dx.doi.org/10.1088/1742-6596/557/1/012020.
[30] A.H. Hosseinloo, K. Turitsyn, Fundamental limits to nonlinear energy harvesting, Phys. Rev. Appl. 4 (6) (2015) 064009, http://dx.doi.org/10.1103/PhysRevApplied.4.064009. (arXiv: 1410.1429v1).
[31] A.H. Hosseinloo, K. Turitsyn, Non-resonant energy harvesting via an adaptive bistable potential, Smart Mater. Struct. 25 (1) (2016) 015010, http://dx.doi.org/10.1088/0964-1726/25/1/015010.
[32] R. Masana, M.F. Daqaq, Response of duffing-type harvesters to band-limited noise, J. Sound Vib. 332 (25) (2013) 6755–6767, http://dx.doi.org/10.1016/j.jsv.2013.07.022.
[33] R.L. Harne, K.W. Wang, A review of the recent research on vibration energy harvesting via bistable systems, Smart Mater. Struct. 22 (2) (2013) 023001, http://dx.doi.org/10.1088/0964-1726/22/2/023001.
[34] R. Masana, M.F. Daqaq, Relative performance of a vibratory energy harvester in mono- and bi-stable potentials, J. Sound Vib. 330 (24) (2011) 6036–6052, http://dx.doi.org/10.1016/j.jsv.2011.07.031.
[35] S.P. Pellegrini, N. Tolou, M. Schenk, J.L. Herder, Bistable vibration energy harvesters: a review, J. Intell. Mater. Syst. Struct. 24 (11) (2013) 1303–1312, http://dx.doi.org/10.1177/1045389X12444940.
[36] S. Zhao, A. Erturk, On the stochastic excitation of monostable and bistable electroelastic power generators: relative advantages and tradeoffs in a physical system, Appl. Phys. Lett. 102 (10) (2013) 103902, http://dx.doi.org/10.1063/1.4795296.
[37] P. Podder, D. Mallick, A. Amann, S. Roy, Influence of combined fundamental potentials in a nonlinear vibration energy harvester, Sci. Rep. 6 (2016) 37292, http://dx.doi.org/10.1038/srep37292.
[38] A. Erturk, D.J. Inman, Issues in mathematical modeling of piezoelectric energy harvesters, Smart Mater. Struct. 17 (6) (2008) 065016, http://dx.doi.org/10.1088/0964-1726/17/6/065016.
[39] M.F. Daqaq, R. Masana, A. Erturk, D.D. Quinn, On the role of nonlinearities in vibratory energy harvesting: a critical review and discussion, Appl. Mech. Rev. 66 (4) (2014) 040801, http://dx.doi.org/10.1115/1.4026278.
[40] H. Goldstein, C.P. Poole, J.L. Safko, Classical Mechanics, Addison Wesley, 2002.
[41] T.K. Caughey, Equivalent linearization techniques, J. Acoust. Soc. Am. 35 (11) (1963) 1706–1711.